Control of a 2-Level System to Reduce Colored Noise

Michael Shalyt

Control of a 2-Level System to Reduce Colored Noise

Research thesis

Submitted in Partial Fulfillment of the Requirements for the degree of Master of Science in Physics

Michael Shalyt

Submitted to Senate of the Technion - Israel Institute of Technology

Shebat, 5773 Haifa January 2013

This research thesis was done under the supervision of Prof. Joseph Avron in the Faculty of Physics.

I would like to thank Prof. Joseph Avron for the opportunity he provided me despite the circumstances, for his spirit and lessons for life.

I would like to thank Dr. Alex Retzker for suggesting the research theme, for his guidance, ideas and care.

I would like to thank Dr. Oded Kenneth for his contributions and unique perspective.

I would like to thank my parents for their support, motivation and love.

I would like to thank the Ulm University for it's hospitality and generous financial support during my visit.

The generous financial support of the Technion and the Israel Science Foundation is gratefully acknowledged.

Contents

List of Figures

Abstract

Quantum computation is one of the most popular and rapidly expanding research topics in past two decades. The possibility of performing tasks that are believed to be unfeasible using classical computation made quantum information wide spread even in popular culture, and there are other - less widely known - applications of pure quantum systems. Unfortunately, experimental realization of a system capable performing even basic calculations is still far from reality. One of the main obstacles is the susceptability to unwanted interaction with the environment (noise) of any quantum system (especially if it is large or for example should act as a measuring apparatus). This interaction causes information stored in the system to "leak" to its sorroundings, thus reducing the system quantum purity (creating decoherence). One possible method of battling this effect is dynamical decoupling (DD) - the use of a deterministic field (control) to act upon the quantum system and effectively reduce the effect of the environment. In the past 15 years dynamical decoupling has proven itself as one of the main methods for maintaining quantum coherence. The DD schemes became increasingly elaborate, the theoretical foundations strengthened and qubit lifetime extension by more than an order of magnitude was measured.

Our research focuses on DD schemes under an energy constraint - a limiting factor mostly ignored in the field until recently. Starting from fundamental principles and using a perturbative approach, we develop a geometric framework for studying a general control scheme for combating noise. We discuss higher perturbation orders - translating the problem to Feynman diagram calculation and proving convergence. We proceed to discuss several specific examples, notably showing entropy reversal. Next we show that decoherence minimization is ill defined without adding constraints and introduce a constraint on the total amount of energy applied to the system. We study the integro-differential equation for constrained optimal control and provide new insights. Using simple geometric and algebraic tools we derive an upper bound on the improvement (decoherence reduction) achievable by any DD scheme constrained by finite energy. We proceed to prove that for the case of square pulses a wide pulse is more efficient in decoupling the system from its environment than a sharp one - in contrast to most of the DD schemes used today. Finally, we show a few limits where a constant control field saturates the improvement bound, making it asymptotically optimal.

List of abbreviations and symbols

List of abbreviations

DD	dynamical decoupling
NMR	nuclear magnetic resonance
CP	Carr and Purcell
CPMG	Carr, Purcell, Meiboom and Gill
PDD	periodic dynamic decoupling
CDD	concatenated dynamic decoupling
UDD	Uhrig dynamic decoupling
QFT	quantum field theory
CF	constant field

List of symbols

$D(t)$	decoherence function
ρ	density matrix
$\vec{r}$	point in Bloch sphere
I	identity matrix
σ_i	the i^{th} Pauli matrix
ϵ_{ijk}	the anti-symmetric tensor
$\mathcal{C}$	quantum channel
λ_i	the i^{th} channel eigenvalue
$\eta(s)$	random field magnitude
$\vec{\Omega}(s)$	control field
$U(t,0)$	unitary operator representing evolution from 0 to t
$\vec{X}(s)$	direction of noise rotation axis in the interaction picture
$\vec{R}(t)$	statistical average of $\vec{r}(t)$
$J(s)$	noise autocorrelation
$\gamma(s,u)$	angle between $\vec{X}(s)$ and $\vec{X}(u)$
$M(s)$	rotation generating matrix
G_z	rotation generator around the $\hat{z}$ axis
$\delta(s)$	Dirac delta function
ν	noise intensity
τ	noise correlation time scale
t	length of evolution time
d	square pulse duration
$\hat{g}(\omega)$	the Fourier transform of $g(t)$
$W_t(s)$	window function

E	maximal allowed energy
λ	Lagrange coefficient
$\vec{X}_r(s)$	time reversed $\vec{X}(s)$ (around $\frac{t}{2}$)

1 Introduction and background

1.1 Quantum purity

The great potential quantum mechanical systems hold for information processing [1, 2] has created increasing interest in quantum information processing over the last two decades. Quantum computers, quantum cryptography and quantum teleportation are some of the most celebrated ideas that emerged in this field, all of them made possible by the fundamental difference between the quantum and classical description of the world [3]. Other applications made possible by coherent control of quantum bits are: quantum sensing in biological systems [4, 5], precise magnetometry [6, 7, 8], and simulation of theories on controlled quantum systems [9, 10], to name a few.

Quantum information processing, as well as other applications, depend on the assumption that the quantum system evolves unitarily in time, under some deterministic Hamiltonian (meaning a closed system). Unfortunately, any physical system is coupled to it's environment (however weakly), so a more accurate way of describing its time evolution is taking into account its open system characteristics. This coupling entangles the system to it's surroundings, a process which transfers information from the system into the surrounding bath - where it is no longer accessible. This non-unitary time propagation of the system, when the state gradually loses it's purity and becomes mixed, is called quantum decoherence [3].

An obvious method to reduce this effect is isolating the system from it's environment as much as possible, but this method is sometimes hard to implement and might create other problems (for example difficulties interacting with the protected system). A more sophisticated way to fight this malicious effect is quantum error correction [11], which can be thought of as a closed-loop (feedback) correction protocol acting on a redundant system [12]. Another possible approach to decoherence reduction is dynamical decoupling (DD): the use of unitary (open-loop) operations on the system to effectively reduce it's coupling to the environment. The fundamental difference between these two strategies is while error correction utilizes the slow rate of the system's decay (so that, with high probability, the amount of information lost to decoherence during the evolution time is no more than the redundancy inserted by the error correcting code), dynamical decoupling uses the assumption that the noise changes slowly - regardless of the system dynamics time scale.

1.2 Hahn echo

Viola and Lloyd [13] introduced dynamical decoupling into quantum information 15 years ago - proposing the use of DD on single qubits (in contrast to spin ensembles). Yet the spin echoes Erwin Hahn measured in NMR systems more than 60 years ago [14] may be considered the true beginning of DD. Hahn used a spin bath immersed in constant magnetic field in the $\hat{z}$ direction, creating level splitting in the spins. Due to the non-homogeneity of the spin bath and magnetic field imperfection, the effective field on each spin is slightly different. This difference in level splitting leads to variations in the Larmor precession frequency, so after a while the magnetic polarization of each spin is different - leading to practically no measurable polarization of the bath. But all is not lost: by applying a π-pulse in the middle of the time evolution this apparent "randomization" of polarizations can be reversed and the bath can be refocused (see Fig. 1). Note that we did not need to know anything about the splitting of any specific spin in order for this method to work.

This effect relies on the assumption that the non-homogenous level splitting does not change during the experiment, if it did then the Larmor precession after the π-pulse would not exactly compensate for the difference in spin directions created before the pulse. This problem can be (at least partially) solved by applying a series of pulses instead of a single one - if the splitting remains practically constant during the interval between subsequent pulses, multiple refocusing "echos" can be measured, as was suggested by Carr and Purcell (CP scheme [15]).

These, relatively simple, methods exemplify the main ideas of dynamical decoupling. The fact that there is no need to know the level splitting of each spin is translated into effectiveness of DD regardless of the specific noise realization. In order to be effective, any DD scheme must act on shorter time scales than the noise correlation - as the CP example shows us.

1.3 DD today

Following the initial publication of the pulsed DD idea ("Bang Bang" control schemes [13]) a significant amount of work has been done in the field. Some additional schemes were assimilated from the field of NMR:

- π-rotations around an axis in the direction of the spin initial state reduce the system sensitivity to pulse inaccuracy (CPMG [16]).
- Different periodic schemes (PDD) were suggested, notably switching the axis of rotation between the X and Y axis every cycle (XY-scheme [17]).

These periodic schemes can be considered as a series of stroboscopic control pulses. The resulting time evolution can be written as a perturbative expansion. A possible measure of the quality of a DD scheme is the maximal expansion order that is negated.

- A concatenated DD scheme (CDD [18]) recursively embeds some pulse pattern into itself, thus eliminating higher orders of the time evolution expansion. The cost of this procedure is an exponentially increasing number of pulses needed to negate high orders of noise.

Thinking of the decoherence as some function $D(t)$ (it will be derived in section 3) that we wish to minimize, an alternative measure of the quality of a DD scheme may be the number of derivatives of $D(t)$ at $t = 0$ that vanish.

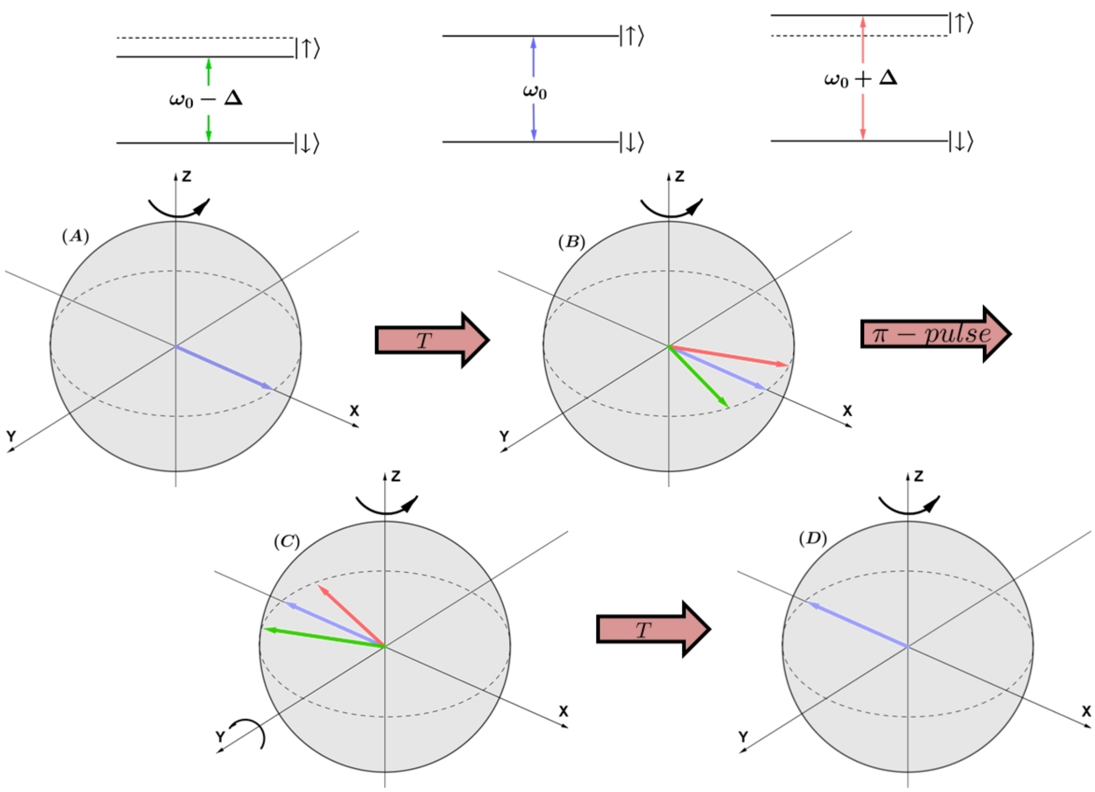

Figure 1: The steps of Hahn echo. (A) At time $t = 0$ all spins are polarized in some direction in the $x - y$ plane. (B) The system undergoes free evolution until $t = T$, during which every spin rotates around the z axis with a Larmor frequency associated with the magnetic field intensity at its site. (C) Using an instantaneous π-pulse, all spins are flipped around the y axis - effectively reversing the direction of rotation. (D) The system again undergoes free evolution for a length of time T, at $t = 2T$ the spin directions coincide once again - hence creating a refocusing effect.

- Uhrig's DD scheme (UDD [19]) uses this vanishing derivative criteria to find the optimal spacing of N pulses, that turns out to be non-equidistant (specifically, for n pulses and total time t, the pulse times t_j are given by: $\frac{t_j}{t} = \sin^2\left(\frac{\pi j}{2n+2}\right)$). This scheme has the advantage of negating higher derivatives using a linearly growing number of pulses.

This scheme was extended and investigated [20, 21], iterated [22] and nested [23] variations were proposed. Yet, since different measures of quality were used to develop the schemes, it should not come as a surprise that neither of them is clearly better - the performance depends on the noise properties [24, 25]. There are quite a few additional schemes suggested in the past few years, both theoretical and experimental work in the quest for most efficient pulse sequence is still in progress (see [26, 27, 28] and references within for recent results). Note that all of the schemes described above assume ideal (instantaneous) pulses in their basic formulation, but the effect of realistic (finite length) pulses was investigated as well (for example in [29, 30]).

So far only pulsed schemes were mentioned. One advantage of sharp pulses is that it reduces the sensitivity of the control scheme to in-homogeneous broadening (as is the case for a spin bath in NMR for example - the field where DD was born) - because the effect created by high intensity field is less sensitive to frequency detuning. Today DD is mostly applied to single qubits (where the detuning can be made negligible) so in general there is no reason why the control field should not change gradually in time. A more general approach was taken in [31, 32], where arbitrary noise spectrum and control modulation were considered. Another reason to introduce non-pulsed schemes is a situation when there is a limitation on the energy allowed to be used in the control field (this is a more strict version of finite control field [33]), in which case ideal pulses are impossible - as their energy approaches infinity. Such a limitation can arise due to heating constraints on the system (for example in quantum sensing of a biological system) or if the applied control field has some errors of its own - since the decoherence induced by this noise is proportional to the intensity of the applied field we want to minimize its total effect [34]. This constraint was first formally introduced in [35] and investigated further in [34].

The main theme of this research is optimal control (DD schemes) under an energy constraint. Our mission is to develop a comprehensible model describing the noise and an arbitrary control field - to serve as a framework for comparing the efficiency of different DD schemes. Next we will attempt to produce and solve an equation describing the optimal control given some noise properties. Finally, we will try to make some broad statements about the effect an energy limitation has on the form and efficiency of a DD scheme.

2 Preliminary definitions

2.1 Bloch sphere

Any density matrix ρ can be written as:

$$\rho = \frac{1}{2}\left(I + \overrightarrow{r} \cdot \overrightarrow{\sigma}\right) \tag{1}$$

Where $\overrightarrow{\sigma} = (\sigma_x, \sigma_y, \sigma_z)$ and

$$\sigma_x = \begin{pmatrix} 0 & 1 \\ 1 & 0 \end{pmatrix},\ \sigma_y = \begin{pmatrix} 0 & -i \\ i & 0 \end{pmatrix},\ \sigma_z = \begin{pmatrix} 1 & 0 \\ 0 & -1 \end{pmatrix} \tag{2}$$

are the Pauli matrices. We will be interested in the 3 dimensional vector $\overrightarrow{r} = (r_x, r_y, r_z)$ that describes the state. The fact that ρ must be positive for any physical state forces $|\vec{r}| \leq 1$ - this set is known as the Bloch sphere.

We will be using the following known identities for Pauli matrices:

$$\begin{aligned}
\vec{\sigma} &= (\sigma_x, \sigma_y, \sigma_z) \\
\sigma_i \cdot \sigma_j &= i \cdot \varepsilon_{ijk} \cdot \sigma_k \\
(\sigma_i)^2 &= I \\
Tr\,(\sigma_i) &= 0 \\
(\overrightarrow{a} \cdot \overrightarrow{\sigma}) \cdot \left(\overrightarrow{b} \cdot \overrightarrow{\sigma}\right) &= \left(\overrightarrow{a} \cdot \overrightarrow{b}\right) I + i\overrightarrow{\sigma} \cdot \left(\overrightarrow{a} \times \overrightarrow{b}\right)
\end{aligned} \tag{3}$$

The definition of the purity of a state described by ρ is [1]:

$$Tr\left[\rho^2\right] = \frac{1}{2}\left(1 + |\overrightarrow{r}|^2\right) \tag{4}$$

So the length of the vector $\vec{r}$ describing a state ρ is a measure of the state purity.

2.2 Quantum channel

A quantum channel $\mathcal{C}$ is a representation of some physical process that takes an initial quantum system ρ_{in} and returns a different state ρ_{out}. Formally, a channel is a completely positive, trace preserving linear map between two spaces of states. The trace preservation and positivity conditions appear trivially from the requirement that ρ_{out} must be a legitimate density matrix (given that ρ_{in} is). The *complete* positivity is due to the fact that the input state might be part of a larger system, and though the channel does not act upon the rest of this system - the resulting composite state must still represent a valid physical system. The definition of complete positivity:

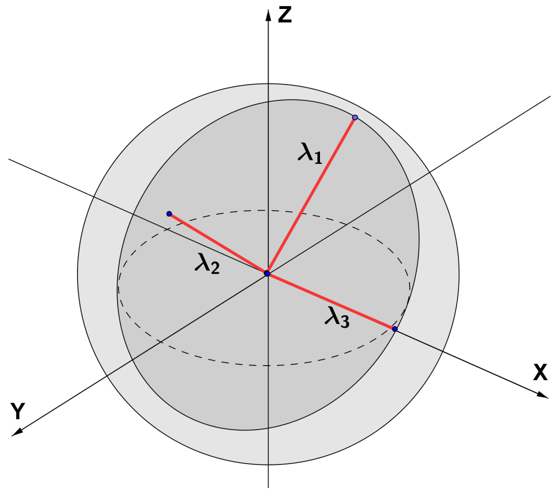

Figure 2: A general channel transforms the Bloch sphere into an ellipsoid inside the sphere. λ_i are the lengths of the semi-axes of the ellipsoid.

given a channel $\mathcal{C}$, $\mathcal{C}_k$ is a positive map for any integer $k \geq 0$, where $\mathcal{C}_k$ is defined as:

$$\mathcal{C}_k = \mathcal{C} \otimes I^k \tag{5}$$

An unbiased channel that does not change the input state if it is maximally mixed ($\mathcal{C}\left[\frac{1}{2}I\right] = \frac{1}{2}I$) is called a unital channel. If we apply such a channel on all pure states (the boundary of the Bloch sphere) the resulting states will form an ellipsoid inside the Bloch sphere (see Fig. 2). This ellipsoid is created by rotating and contracting the Bloch sphere surface. From equation 4 it is obvious that the rotation part of this transformation does not change the purity of the affected system, while the contraction reduces it (introducing decoherence).

Due to the complete positivity condition, not any sphere contraction is allowed. After some simple manipulations, the result in [36] can be transformed into the following inequalities that the ellipsoid semi-axes lengths λ_i must fulfill (besides the trivial $|\lambda_i| \leq 1$):

$$\begin{aligned} |\lambda_1 - \lambda_2| &\leq |1 - \lambda_3| \\ |\lambda_1 + \lambda_2| &\leq |1 + \lambda_3| \end{aligned} \tag{6}$$

These inequalities can be drawn in the $\lambda_1 - \lambda_2 - \lambda_3$ space using the following "Mathematica" code[1]:

```
ContourPlot3D[{Abs[x + y] == Abs[1 + z], Abs[x - y] == Abs[1 - z]},
{x, -1, 1}, {y, -1, 1}, {z, -1, 1},   Mesh -> None]
```

[1]Throughout this work we present the relevant code for calculating tedious integrals or plots instead of tiring the reader with long technical derivations

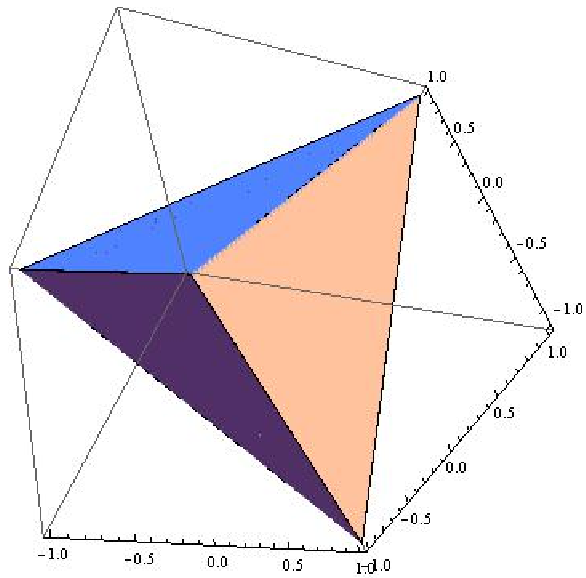

Figure 3: The possible values for the eigenvalues of a completely positive quantum channel (λ_i) form a tetrahedron in the $\lambda_1 - \lambda_2 - \lambda_3$ space.

Where they define a tetrahedron (see Fig. 3).

3 Model and decoherence function

We think of a qubit initialized in some state that is being influenced by some malicious random field $\eta(t)$ that creates decoherence (note that we model the noise as a classical random field - which is usually the case in experimental setups - and not as a quantum mechanism of information transfer out of the system). Additionally, a deterministic field is applied on the qubit, creating some controlled rotation of the Bloch sphere. The goal is to reduce the effect of $\eta(t)$ using the deterministic (control) field. This theoretical qubit is implemented in reality by a two level system that has an energy gap (natural or artificially created) and is being irradiated by a resonant electromagnetic field, creating said rotation. The ambient noise acts on the two level system in all directions, but only noise in the z-axis direction has a significant affect (the other directions don't preserve energy). Combining these observations and translating the problem into the interaction picture (in respect to the rotation created by the energy gap) we get the Hamiltonian:

$$H(t) = \frac{1}{2}\hbar\eta(t)\sigma_z + \frac{1}{2}\hbar\vec{\Omega}(t)\cdot\vec{\sigma} \tag{7}$$

We think of $\eta(t)$ as a stationary, unbiased ($\langle\eta(t)\rangle = 0$), random process representing noise and of $\vec{\Omega}(t)$ as the control field. Moving into the interaction picture (once more) in respect to the $\frac{1}{2}\hbar\vec{\Omega}(t)\cdot\vec{\sigma}$ part (defining $H_0(t) = \frac{1}{2}\hbar\vec{\Omega}(t)\cdot\vec{\sigma}$ and $H_1(t) = \frac{1}{2}\hbar\eta(t)\sigma_z$ the Hamiltonian in the interaction picture is $H_I(t) = U_0^\dagger(t,0)\cdot H_1\cdot U_0(t,0)$, where $U_0(t,0)$ is the time evolution operator with respect to H_0), we get the Hamiltonian in this frame:

$$H_I(t) = \frac{1}{2}\hbar\eta(t)\vec{X}(t)\cdot\vec{\sigma} \tag{8}$$

$\vec{X}(t)$ is defined by $\vec{\Omega}(t)$ via the relation ($\vec{X}(0) = \hat{z}$ of course):

$$\vec{X}(t+dt)\cdot\vec{\sigma} = \exp\left(i\frac{1}{2}\Omega\vec{(t)}\cdot\vec{\sigma}dt\right)\vec{X}(t)\cdot\vec{\sigma}\exp\left(-i\frac{1}{2}\Omega\vec{(t)}\cdot\vec{\sigma}dt\right) \tag{9}$$

$$\dot{\vec{X}}(t)\cdot\vec{\sigma} = \frac{i}{2}\left[\left(\Omega\vec{(t)}\cdot\vec{\sigma}\right)\left(\vec{X}(t)\cdot\vec{\sigma}\right) - \left(\vec{X}(t)\cdot\vec{\sigma}\right)\left(\Omega\vec{(t)}\cdot\vec{\sigma}\right)\right] \tag{10}$$

Using equation 3 this can be brought to the form:

$$\dot{\vec{X}}(t) = \vec{X}(t)\times\vec{\Omega}(t) \tag{11}$$

Now we can calculate the time evolution equation for a state density matrix (using the Bloch sphere notation - equation 1):

$$\begin{aligned}\dot{\rho} &= \frac{-i}{\hbar}[H,\rho] \\ \dot{\vec{r}}(t) &= \eta(t)\vec{X}(t)\times\vec{r}(t)\end{aligned} \tag{12}$$

Since $\vec{r}(t)$ is stochastic (due to it's dependance on the stochastic $\eta(t)$), the density matrix describing the physical state is defined by the average vector:

$$\vec{R}(t) = \langle\vec{r}(t)\rangle$$

Equation 12 generates some time evolution of $\vec{R}$. We can think of this evolution as a quantum channel that propagates the initial state in time: $\vec{R}(t) = \mathcal{C}(t)\left[\vec{R}(0)\right]$.

There is no single all encompassing definition of a channel's quality. Instead, a more practical approach is taken - the quality of a channel depends on its intended use. As we are interested in preserving the purity of an unknown initial state, we must take into account the channel's action on all possible initial states. One possible measure of the decoherence a channel introduces that considers the whole Bloch sphere is:

$$D(\mathcal{C}) = \sum_{i=1}^{3} 1 - |\lambda_i| \tag{13}$$

Where λ_i are the channel eigenvalues. If all eigenvalues are 1 the channel is purely rotating so it introduces no decoherence - see section 2.

3.1 Perturbative representation

We now use the definition of decoherence in equation 13 and perturbation theory up to second order in $\eta(t)$ (higher orders will be discussed in section 4) to obtain an explicit expression for $D(t)$.

We expand $\vec{r}(t)$ in respect to powers of $\eta(t)$ as:

$$\vec{r}(t) = \sum_{n=0}^{\infty} \vec{r}_n(t) \tag{14}$$

Remembering that $\langle \eta(t) \rangle = 0$ (and using equation 12) we get:

$$\begin{array}{lccr} \eta^0: & \dot{\vec{r}}_0(t) = 0 & \Longrightarrow & \vec{R}_0(t) = \vec{r}(0) \\ \eta^1: & \dot{\vec{r}}_1(s) = \eta(s)\vec{X}(s) \times \vec{r}_0(s) & \Longrightarrow & \vec{R}_1(t) = \int_0^t \langle \eta(s) \rangle \vec{X}(s) \times \vec{r}(0)\, ds = 0 \\ \eta^2: & \dot{\vec{r}}_2(s) = \eta(s)\vec{X}(s) \times \vec{r}_1(s) & \Longrightarrow & \vec{R}_2(t) = \int_0^t \int_0^s \langle \eta(s)\eta(u) \rangle \vec{X}(s) \times \left[\vec{X}(u) \times \vec{r}(0)\right] dsdu \end{array} \tag{15}$$

Leading to the quantum channel:

$$\begin{aligned} \mathcal{C}(t)\left[\vec{R}\right] &= \vec{R} + \int_0^t \int_0^s \langle \eta(s)\eta(u) \rangle \vec{X}(s) \times \left(\vec{X}(u) \times \vec{R}\right) duds = \\ &= \vec{R} + \int_0^t \int_0^s \langle \eta(s)\eta(u) \rangle \left[\left(\vec{X}(s) \cdot \vec{R}\right)\vec{X}(u) - \left(\vec{X}(s) \cdot \vec{X}(u)\right)\vec{R}\right] duds \end{aligned} \tag{16}$$

Using this channel we calculate explicitly the decoherence as a function of time (see appendix A for derivation):

$$D(t) = 2\int_0^t \int_0^s \langle \eta(s)\eta(u) \rangle \vec{X}(s) \cdot \vec{X}(u)\, duds \tag{17}$$

Defining the autocorrelation function $J(s-u) = \langle \eta(s)\eta(u) \rangle$, remembering that $\left|\vec{X}(s)\right| = 1$, defining $\gamma(s,u)$ as the angle between $\vec{X}(s)$ and $\vec{X}(u)$ and using symmetry under exchanging s and u, we get:

$$D(t) = \int_0^t \int_0^t J(s-u)\cos(\gamma(s,u))\, duds \tag{18}$$

This formula can be represented geometrically as pictured in Fig. 4. Note that if we assume $J(s)$ is monotonically decreasing with s, then *any* control field reduces the decoherence compared to no control.

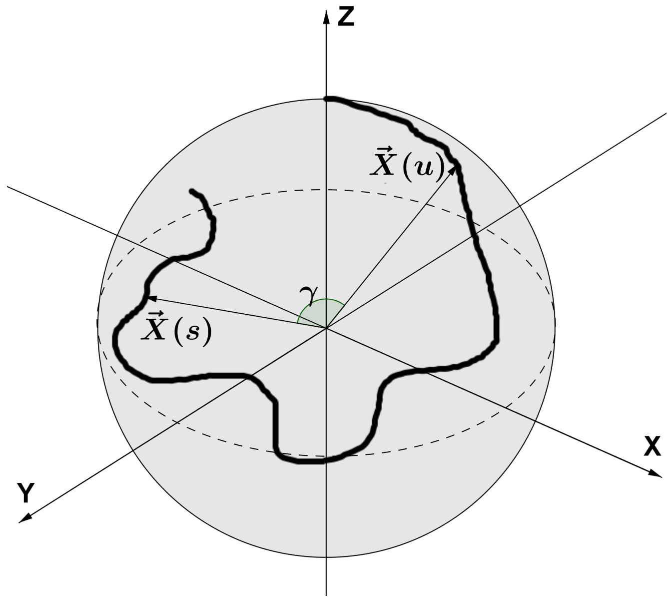

Figure 4: A geometric interpretation of equation 18. $\vec{X}(s)$ rotates due to the applied control field and traces some path on the Bloch sphere (wide black line) during the time $0 \to t$. The decoherence is determined by going over all possible pairs of points on this path and summing the cosine of the angle between them multiplied by the autocorrelation between these times.

4 Higher perturbation orders

In this section we discuss the higher perturbation orders that we neglected in section 3. We translate the perturbative calculation into Feynman diagrams, show that the series converge and calculate the order of magnitude of the n^{th} order. From equation 12 we can write an expression for the n^{th} order in perturbation theory:

$$\vec{R}_n(t) = \int_0^t \int_0^{s_1} \dots \int_0^{s_{n-1}} \langle \eta(s_1) \dots \eta(s_n) \rangle \left(\vec{X}(s_1) \times \dots \times \left(\vec{X}(s_{n-1}) \times \left(\vec{X}(s_n) \times \vec{r}(0) \right) \right) \right) ds_1 \dots ds_n \tag{19}$$

Assuming $\eta(s)$ is a Gaussian process and remembering that $\langle \eta(s) \rangle = 0$ we can use Isserlis' theorem [37] (the mathematical origin of Wick's theorem from quantum field theory [38]):

$$\langle \eta(s_1) \dots \eta(s_n) \rangle = \begin{cases} 0 & n\,odd \\ \sum \prod_{i-k\ pairings} \langle \eta(s_i)\, \eta(s_k) \rangle & n\,even \end{cases} \tag{20}$$

Where the sum is over all possible multiplications of pair-wise correlations (contractions in QFT). Since $\langle \eta(s_i)\, \eta(s_k) \rangle = J(s_i - s_k)$ is known, it is theoretically possible to calculate $\vec{r}(t)$ up to any order. Defining $\vec{X}(t) \times \vec{r} = M(t)\, \vec{r}$ and using the symmetry of the integrand we can write (T

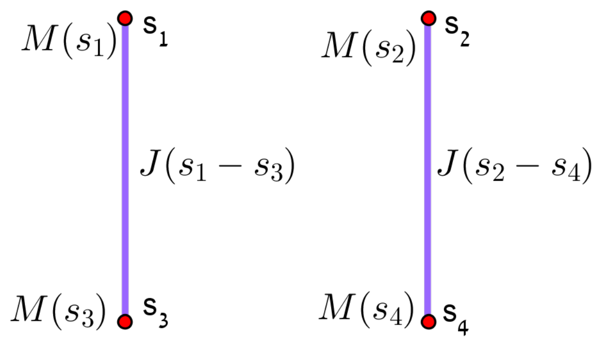

Figure 5: One of three Feynman diagrams for a 4-th order perturbative correction.

represents time ordering):

$$\vec{R}_n(t) = \frac{1}{n!} \int_0^t \int_0^t \ldots \int_0^t \langle \eta(s_1) \ldots \eta(s_n) \rangle \, \mathrm{T} M(s_1) \ldots M(s_{n-1}) \, M(s_n) \, \vec{r}(0) \, ds_1 \ldots ds_n \qquad (21)$$

Associating vertices with $M(s_i)$ and propagators with $J(s_i - s_k)$ we have translated the calculation into Feynman diagrams (see Fig. 5 for an example).

As always when dealing with Feynman diagrams, a crucial point is the question of the series convergence. The number of diagrams (which is the number of possible ways to contract n members into pairs) for the n^{th} order is (n is even or the contribution is 0):

$$\frac{n!}{2^{\frac{n}{2}} \left(\frac{n}{2}\right)!} \qquad (22)$$

Since both $J(s_i - s_k)$ and $M(s_i)$ are bound from above for any values of s (J due to the fact that the noise intensity is finite and M as a rotation generator), the $\frac{1}{n!}$ coefficient in equation 21 makes sure the sum is finite with an infinite convergence radius.

Assuming $\langle \eta(s_i) \, \eta(s_k) \rangle = J(s_i - s_k)$ has a typical width τ, we can asses $|\vec{r}_n(t)|$:

$$|\vec{r}_n(t)| \lesssim \left(\left\langle \eta^2(s) \right\rangle t\tau \right)^{\frac{n}{2}} \qquad (23)$$

Where $\left\langle \eta^2(s) \right\rangle$ is the small parameter.

5 Uncontrolled stochastic evolution

In this section we calculate the exact expression for decoherence without any control field and show that it rises slowly (sublinearly) for short times and linearly for longer times. The no control case can be solved exactly (non-perturbatively). Since $\vec{\Omega} = 0$, it follows from equation 11 that

$\vec{X}(t) = \hat{z}$, so the equation of motion for $\vec{r}$ is simply (using equation 12):

$$\dot{\vec{r}}(t) = \eta(t)\,\hat{z} \times \vec{r}(t) \tag{24}$$

Defining the rotation generator around the $\hat{z}$ axis (G_z) we get:

$$G_z = \begin{pmatrix} 0 & 1 & 0 \\ -1 & 0 & 0 \\ 0 & 0 & 0 \end{pmatrix} \tag{25}$$

$$\begin{aligned} \dot{\vec{r}}(t) &= \eta(t)\, G_z \vec{r}(t) \Longrightarrow \\ \vec{r}(t) &= e^{G_z \int_0^t \eta(s)ds} \vec{r}(0) \end{aligned} \tag{26}$$

Under the assumption from section 4 that $\eta(s)$ is Gaussian, we can calculate $\vec{R}$:

$$\vec{R} = \left\langle e^{G_z \int_0^t \eta(s)ds} \vec{r}(0) \right\rangle = e^{\frac{1}{2}(G_z)^2 \left\langle \left(\int_0^t \eta(s)ds\right)^2 \right\rangle} \vec{r}(0) \tag{27}$$

$$(G_z)^2 = \begin{pmatrix} -1 & 0 & 0 \\ 0 & -1 & 0 \\ 0 & 0 & 0 \end{pmatrix} \tag{28}$$

$$\left\langle \left(\int_0^t \eta(s)\, ds \right)^2 \right\rangle = \int_0^t \int_0^t \langle \eta(s)\, \eta(u) \rangle\, duds \tag{29}$$

5.1 White noise

Choosing $\eta(s)$ to be white noise ($J(s-u) = 2a\delta(s-u)$) its easy to solve for $\vec{R}$:

$$\vec{R}_x(t) = e^{-at}\vec{r}_x(0) \quad \vec{R}_y(t) = e^{-at}\vec{r}_y(0) \quad \vec{R}_z(t) = \vec{r}_z(0) \tag{30}$$

So the state purity decays exponentially (as is often assumed to be the case).

5.2 Colored noise

Now we choose non-Markovian noise statistics: $J(s) = \nu^2 e^{-\frac{|s|}{\tau}}$ (ν is the noise intensity), meaning a Lorentzian noise spectrum - as predicted for a spin bath by Anderson [39]. Using the following "Mathematica" code:

```
Integrate[2*Exp[-(s - u)/τ], {s, 0, t}, {u, 0, s}]  ⟹
⟹ 2τ(t + (-1 + E^(-(t/τ)))τ)
```

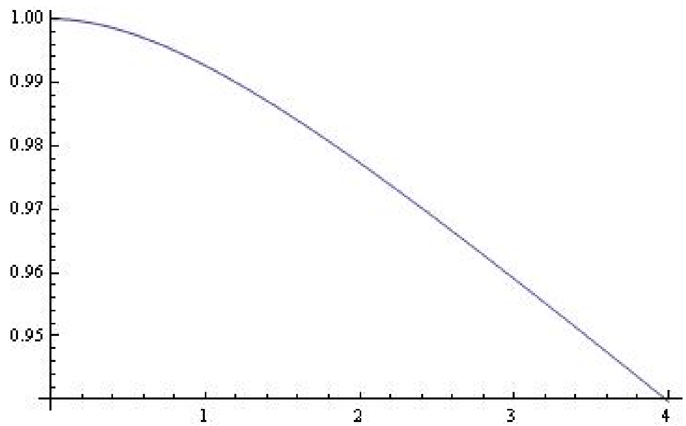

Figure 6: $\frac{|\vec{R}(t)|}{|\vec{R}(0)|}$ vs. $t \in [0\,,\,4\tau]$. For $t \lesssim \tau$ the state purity is decaying slower than linearly.

We get a more complicated behavior of $\vec{R}\,(t)$:

$$\int_0^t \int_0^t J\,(s-u)\,duds = 2\nu^2\tau\left(t - \tau + \tau e^{-\frac{t}{\tau}}\right) \tag{31}$$

$$\vec{R}_x\,(t) = e^{-2\nu^2\tau\left(t-\tau+\tau e^{-\frac{t}{\tau}}\right)}\vec{r}_x\,(0) \quad \vec{R}_y\,(t) = e^{-2\nu^2\tau\left(t-\tau+\tau e^{-\frac{t}{\tau}}\right)}\vec{r}_y\,(0) \quad \vec{R}_z\,(t) = \vec{r}_z\,(0) \tag{32}$$

Assuming $\vec{r}\,(0)$ is in the $x-y$ plane we can draw $\frac{|\vec{R}(t)|}{|\vec{R}(0)|}$ as a function of time (see Fig. 6) and see that for small t ($t \sim \tau$) the decay is sublinear - slowly rising.

An alternative way to see this result is using equation 18 (setting $\gamma = 0$ as there is no control field) and taking the limit of $\frac{t}{\tau} \ll 1$:

$$D_{free}\,(t) = \nu^2\tau^2\left(\frac{t}{\tau}\right)^2 = \nu^2 t^2 \tag{33}$$

Where we see that the decoherence rises as the square of the time for short times, no linear term.

Taking the opposite limit ($\frac{t}{\tau} \gg 1$) of equation 18 we get:

$$D_{free}\,(t) = 2\nu^2\tau^2 \cdot \frac{t}{\tau} \tag{34}$$

A linearly increasing function with t - as we would expect from Fig. 6.

6 Solvable control models

6.1 White noise

First, we show that dynamical decoupling is ineffective against white noise. Let us assume a thermodynamic (steady state) bath. This memory-less bath is translated to noise correlation function $J(s-u) \propto \delta(s-u)$:

$$D(t) \propto \int_0^t \int_0^t \delta(s-u)\cos(\gamma(s,u))\, duds = \int_0^t \cos(0)\, ds \tag{35}$$

Which is equivalent to zero control field (free evolution), so for a memory-less bath (white noise) no DD has any effect - showing once again the importance of noise correlation length to the success of DD schemes.

6.2 Hahn echo

In this section we give a geometric interpretation of Hahn echo. More surprisingly, we will see that this seemingly simple control scheme reverses the flow of entropy for a short time. Taking the control field to be a π-pulse at $\frac{t}{2}$ and fixing $\hat{\Omega}$ in the $x-y$ plane, we can use the following "Mathematica" code to get (assuming the same Lorentzian noise spectrum as in section 5):

```
Simplify[
Integrate[2*Exp[-(s - u)/τ], {s, 0, t/2}, {u, 0, s}] +
Integrate[2*Exp[-(s - u)/τ], {s, t/2, t}, {u, t/2, s}] -
Integrate[2*Exp[-(s - u)/τ], {s, t/2, t}, {u, 0, t/2}]] ⟹
⟹ 2 τ (t + (-3 - E^(-(t/τ)) + 4 E^(-(t/(2 τ)))) τ)
```

$$D_{Hahn}(t) = 2\nu^2\tau^2\left(\frac{t}{\tau} + 4\exp\left(-\frac{1}{2}\frac{t}{\tau}\right) - \exp\left(-\frac{t}{\tau}\right) - 3\right) \tag{36}$$

Taking the limit of $\frac{t}{\tau} \ll 1$ (a fast pulse) we get:

$$D_{Hahn}(t) = \frac{1}{6}\nu^2\tau^2\left(\frac{t}{\tau}\right)^3 \tag{37}$$

Which shows that for very short time lengths the decoherence rises as the cube of the time, so Hahn echo negated the leading order of the decoherence accumulation under free evolution - which is the fundamental idea behind "bang bang" control (assuming we periodically apply a π-pulse every time $t \ll \tau$). Note that this term is still much larger than the next order of perturbation theory for sufficiently small ν (see equation 23):

$$\frac{t}{\tau} \gg \nu^2\tau^2 \Longrightarrow$$

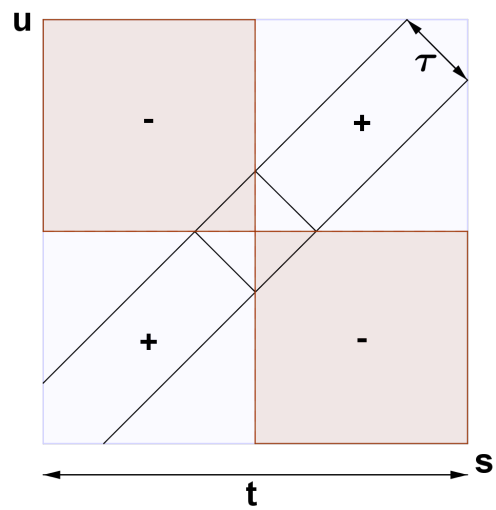

Figure 7: $s-u$ plane with a π pulse at $\frac{t}{2}$. Width of correlation function $J\left(s-u\right)\left(\tau\right)$ and $\cos\left(\gamma\left(s,u\right)\right)$ are drawn. The square (of size $\sim\tau^2$) in the middle is canceled due to the sign change caused by the pulse, so the effective lifetime is prolonged by $\sim\tau$ (specifically 2τ).

$$\nu^2\tau^2\left(\frac{t}{\tau}\right)^3 \gg \nu^4\tau^2t^2 \tag{38}$$

So this result is within the scope of second order perturbation theory.

Taking the opposite limit of $\frac{t}{\tau}\gg 1$ (using equation 31) we see that a single pulse prolongs the lifetime of the qubit by 2τ:

$$D_{free}\left(t\right) = D_{Hahn}\left(t+2\tau\right) \tag{39}$$

This can be understood using a drawing - as shown in Fig.7.

Using the code:

```
tau = 1
T = 8*tau
int = 0.1
Plot[1 - NIntegrate[2*int^2*(1 - 2*UnitStep[s-T/2,T/2-u])*Exp[-(s-u)/tau],
{s, 0, t}, {u, 0, s}], {t, 0, T}]
```

We plot $1-D_{Hahn}\left(s\right)$ in the interval $\left[0\,,\,t\right]$. A "bump" can be seen on the graph - starting at the time of the pulse (see Fig. 8). This "bump" shows that by applying a unitary operation it is possible to create a time interval during which the purity of the qubit increases. Since a qubit's purity is correlated to it's entropy, during the first half of the "bump" the *flow of entropy is reversed* - seemingly violating the second law of thermodynamics. This "paradox" is resolved by looking at the result in section 6.1, clearly showing that this "violation" is made possible due to the noise memory properties and the smallness of the system.

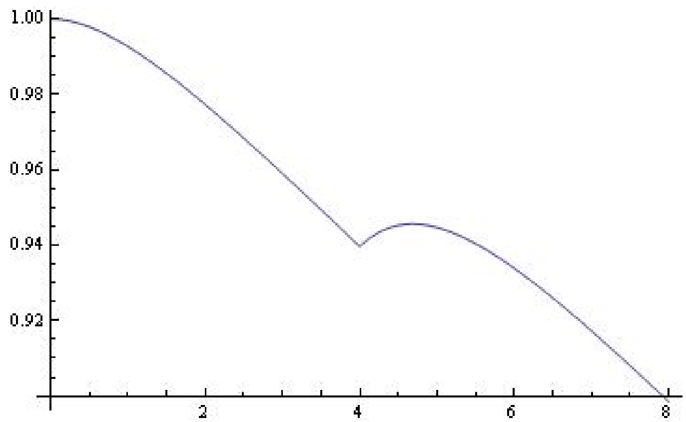

Figure 8: $1 - D(s)$ plotted for $s \in [0, t]$ with a π-pulse applied at $\frac{t}{2}$. Note that right after the pulse the decoherence decreases.

This example contradicts the claim in [35] that dynamic decoupling does not contain an entropy removal mechanism.

6.3 Constant field

In this section we take the an approach that is in a sense opposite to pulsed DD schemes - we use a constant control field (CF) that drives the system with fixed angular velocity (again fixing $\hat{\Omega}$ in the $x-y$ plane and using the same noise autocorrelation as before). The driven system can be said to have dressed states with a different energy splitting than the original, and this "new" two level system is less susceptible to the ambient noise - as proposed and shown experimentally in [40]. For $\Omega = const$ we can use the following "Mathematica" code to get (see Fig.9 for a visualization of the integral):

```
Simplify[
 Integrate[ 2*Exp[-(s - u)/τ]*Cos[m*(s - u)], {s, 0, t}, {u, 0, s}]] ⟹
⟹ (2 E^(-(t/τ)) τ (E^(t/τ) (t - τ + m^2 t τ^2 + m^2 τ^3) +
(τ -m^2 τ^3) Cos[m t] - 2 m τ^2 Sin[m t]))/(1 + m^2 τ^2)^2
```

$$D_{CF}(t) = \frac{2\nu^2}{\left((\Omega\tau)^2+1\right)^2}\left(\left(1+(\Omega\tau)^2\right)t\tau + \right.$$
$$\left. +\tau^2\left(1-(\Omega\tau)^2\right)\left(\exp\left(-\frac{t}{\tau}\right)\cos(\Omega t)-1\right) - 2\Omega\tau^3\exp\left(-\frac{t}{\tau}\right)\sin(\Omega t)\right) \quad (40)$$

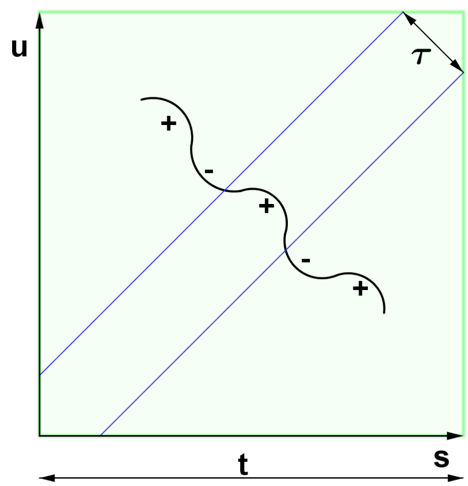

Figure 9: $s-u$ plane with a CF control field. The phase fluctuations (drawn as a black wave) reduce the decoherence due to partial cancellation of the noise sum caused by the cosine fluctuations.

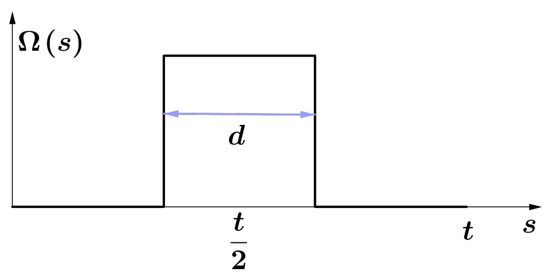

Figure 10: Intensity of control field as a function of time for a square pulse DD scheme.

For $\frac{t}{\tau} \gg 1$ this formula is greatly simplified:

$$D_{CF}(t) = \frac{2\nu^2}{\left((\Omega\tau)^2 + 1\right)} t\tau \tag{41}$$

$$\frac{D_{CF}(t)}{D_{free}(t)} = \frac{1}{\left((\Omega\tau)^2 + 1\right)} \tag{42}$$

So the rate of decoherence accumulation is reduced by a factor that scales with the number of cycles the control field induces during τ: $\sim \Omega\tau$. The stronger the field - the more cycles are induced - and the longer the qubit lifetime is extended.

6.4 Square pulse

As a last example we take a control field shaped as a square pulse of width d and constant height Ω centered at $\frac{t}{2}$ (once again fixing $\hat{\Omega}$ in the $x-y$ plane and using the same noise statistics) - as drawn in Fig. 10. We will show that the decoherence under this control is simply a linear combination of decoherence caused by free evolution for time $t-d$ and CF control for time d. Using the following "Mathematica" code (and algebraic manipulations on the 4 line output generated by it) we get:

```
Simplify[
Integrate[2*Exp[-(s - u)/τ], {s, 0, (t - d)/2}, {u, 0, s}] +
Integrate[2*Exp[-(s - u)/τ], {s, (t + d)/2, t}, {u, (t + d)/2, s}] -
Integrate[2*Exp[-(s - u)/τ], {s, (t + d)/2, t}, {u, 0, (t - d)/2}] +
Integrate[2*Exp[-(s - u)/τ]*Cos[m*(s - u)], {s, (t - d)/2, (t + d)/2},
{u, (t - d)/2, s}] +
Integrate[2*Exp[-(s - u)/τ]*Cos[m*(s - (t - d)/2)], {s, (t - d)/2, (t + d)/2},
{u, 0, (t - d)/2}] +
Integrate[2*Exp[-(s - u)/τ]*Cos[m*(d - (u - (t - d)/2))], {s, (t + d)/2,t},
{u, (t - d)/2, (t + d)/2}]]
```

$$\begin{aligned}D_{pulse}\left(d,t\right) &= 2\nu^2\tau^2\left[\frac{(t-d)}{\tau}+\frac{1}{\left(1+\left(\Omega\tau\right)^2\right)}\frac{d}{\tau}+\right.\\ &+\exp\left(-\frac{d}{\tau}\right)\left(\cos\left(\Omega d\right)-\frac{2\sin\left(\Omega d\right)}{\left(1+\left(\Omega\tau\right)^2\right)}\left(\sin\left(\Omega\frac{t-d}{2}\right)+\right.\right.\\ &\left.\left.\left.+\ \Omega\tau\cos\left(\Omega\frac{t-d}{2}\right)\right)\right)\right]\end{aligned} \quad (43)$$

Assuming the pulse is much wider than the bath memory $\frac{d}{\tau}\gg 1$ the expression is simplified to:

$$D_{pulse}\left(d,t\right)=2\nu^2\tau^2\left(\frac{(t-d)}{\tau}+\frac{1}{\left(1+\left(\Omega\tau\right)^2\right)}\frac{d}{\tau}\right) \quad (44)$$

Which is a linear combination of equations 34 and 41, as we set out to prove. This can also be seen from the corresponding $s-u$ plane drawing (Fig. 11).

7 Unconstrained control

In this section we will show that the general problem of dynamical decoupling without any limitations on the control is ill defined: the decoherence can be made arbitrarily small - but the control function becomes increasingly "bad". For that end we first translate the decoherence function (equation 18) to the frequency domain. Limiting the applied field ($\vec{\Omega}\left(t\right)$) to a fixed direction in

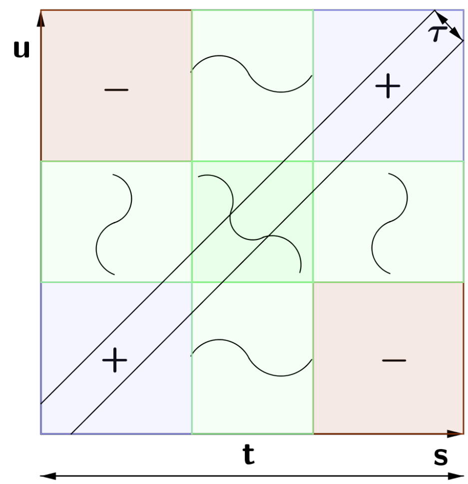

Figure 11: $s-u$ plane with a wide pulse control field. Decoherence is reduced in the central green square and is left unchanged in the blue $(+)$ squares.

the $x-y$ plane, we force $\vec{X}$ to rotate on a great circle - so the angle γ is given by:

$$\gamma\left(s,u\right)=\int_{u}^{s}\Omega\left(t\right)d\tau \tag{45}$$

Where $\Omega\left(t\right)=\left|\vec{\Omega}\left(\tau\right)\right|$. Defining the Fourier transform as:

$$\hat{g}\left(\omega\right)=\frac{1}{\sqrt{2\pi}}\int_{-\infty}^{\infty}g\left(\tau\right)e^{-i\omega\tau}d\tau \tag{46}$$

Using a window function (W_t) and assuming $J\left(s\right)$ is square integrable we rewrite equation 18 as:

$$W_t\left(s\right)=\begin{cases}0 & s<0\\ 1 & 0<s<t\\ 0 & t<s\end{cases} \tag{47}$$

$$f_t\left(s\right)=W_t\left(s\right)\cdot e^{i\int_0^s\Omega(\tau)d\tau} \tag{48}$$

$$D\left(t\right)\;=\;\Re\left[\int_{-\infty}^{\infty}\int_{-\infty}^{\infty}J\left(s-u\right)f_t\left(s\right)\overline{f_t}\left(u\right)duds\right] \tag{49}$$

Transforming into the frequency representation we get (see appendix B for derivation):

$$D(t) = \sqrt{2\pi} \int_{-\infty}^{\infty} \hat{J}(\omega) \left| \hat{f}_t(\omega) \right|^2 d\omega \tag{50}$$

This is the decoherence rate spectral formula from [31], derived from simple Fourier considerations. An immediate result of this form is that $D(t)$ is always positive. $\left|\hat{f}_t(\omega)\right|^2$ can be thought of as a filter function (that is determined by the applied control field $\Omega(t)$) and of $\hat{J}(\omega)$ as some noise the filter should block, the decoherence minimization challenge transforms into a filer design problem (this idea was explored in [24]).

If the control field is constant ($\Omega(t) = \Omega$), $\left|\hat{f}_t(\omega)\right|^2$ can be calculated exactly:

$$\left|\hat{f}_t(\omega)\right|^2 = \left|\frac{1}{\sqrt{2\pi}} (\hat{W_t}(s)) * (\widehat{e^{i\Omega s}})\right|^2 = \frac{1}{\pi^2} \frac{\sin^2\left(\frac{(\omega-\Omega)t}{2}\right)}{(\omega-\Omega)^2} \tag{51}$$

Which is simply a sinc function of width $\frac{1}{t}$ (due to the time window) centered at Ω (due to the control field). Since $J(s)$ is square integrable, $\hat{J}(\omega)$ is square integrable as well - so obviously:

$$\lim_{\omega\to\infty} \hat{J}(\omega) = 0 \tag{52}$$

So if we take Ω to be large enough, the sinc will be centered at a frequency where $\hat{J}(\omega)$ is arbitrarily small, hence:

$$\lim_{\Omega\to\infty} D(t) = 0 \tag{53}$$

We see that a constant control field (in magnitude and direction) is enough to make the decoherence arbitrarily small - if the field is allowed to be sufficiently strong. As Ω goes to infinity, the $e^{i\Omega s}$ function becomes increasingly “bad” (all it’s derivatives go to infinity), making this question an ill defined optimization problem.

8 Energy constraint

After seeing in section 7 that the unbound optimization problem is ill defined, we introduce a constraint on the total energy of the control field:

$$\int_0^t \left|\vec{\Omega}(s)\right|^2 ds \leq E \tag{54}$$

This translates to a limitation on $\vec{X}(s)$ (using equation 11) as:

$$\int_0^t \left|\dot{\vec{X}}(s)\right|^2 ds \leq \int_0^t \left|\vec{\Omega}(s)\right|^2 ds \leq E \tag{55}$$

So we can substitute the problem of finding the optimal control field $\vec{\Omega}(t)$ by considering $\vec{X}(t)$ as the control vector (as it is fully defined by $\vec{\Omega}(t)$) and get the following constrained minimization problem:

$$\begin{cases} \min_{\vec{X}} D(t) \\ \left|\vec{X}\right| = 1 \\ \int_0^t \left|\dot{\vec{X}}(s)\right|^2 ds \leq E \end{cases} \tag{56}$$

Using variational calculus we get the following integro-differential equation for optimal control (see appendix C for derivation):

$$\vec{X}(s) \times \left[\int_0^t J(s-u)\,\vec{X}(u)\,du - \lambda \ddot{\vec{X}}(s)\right] = 0 \tag{57}$$

$$\vec{X}(0) \times \dot{\vec{X}}(0) = \vec{X}(t) \times \dot{\vec{X}}(t) = 0$$

λ is chosen such that the resulting $\vec{X}$ fulfills the energy restriction. This is a non-linear integro-differential equation, making it in general a hard problem.

An important property of this equation is that if $\vec{X}(s)$ is a solution then if we reverse it in time ($\vec{X}_r(s) = \vec{X}(t-s)$) we get a valid solution as well:

$$\vec{X}_r(s) \times \left[\int_0^t J(s-u)\,\vec{X}_r(u)\,du - \lambda \ddot{\vec{X}}_r(s)\right] =$$

$$\{\tilde{s} = t - s \;\; \tilde{u} = t - u\}$$

$$\vec{X}(\tilde{s}) \times \left[\int_t^0 J(\tilde{s}-\tilde{u})\,\vec{X}(\tilde{u})\,(-d\tilde{u}) - \lambda(-1)^2\, \ddot{\vec{X}}(\tilde{s})\right] =$$

$$\vec{X}(\tilde{s}) \times \left[\int_0^t J(\tilde{s}-\tilde{u})\,\vec{X}(\tilde{u})\,d\tilde{u} - \lambda \ddot{\vec{X}}(\tilde{s})\right] = 0 \tag{58}$$

And the boundary conditions are trivially fulfilled. If this equation has a unique solution, this property forces it to be symmetric around $\frac{t}{2}$:

$$\vec{X}(s) = \vec{X}(t-s) \tag{59}$$

A similar result was given in [35] by Goren, Kurizki and Lidar, but there are several important differences. First, they assume $\vec{\Omega}(t)$ to be in a fixed direction while we allow for the general case. Second, only one boundary condition was enforced in their version ($\dot{\vec{X}}(0) = 0$), missing the condition on $\dot{\vec{X}}(t)$. Third, they calculate numerical solutions of their equation for several specific noise spectra and claim that this solution is unique - yet it is not symmetric around $\frac{t}{2}$, in violation of equation 59.

9 Coherence gain upper bound

Now we will show that the energy constraint imposes a restriction on the efficiency of a DD scheme. This is done by deriving an upper bound on the coherence gain (versus no control field) - ΔD - under an energy constraint E. The work in this section was done in collaboration with Dr. Oded Kenneth.

Using the trivial geometric fact that the length of any path is longer than the distance between it's end points and Cauchy–Schwarz inequality we write:

$$\gamma(s,u) \leq \int_u^s \left|\dot{\vec{X}}(\tau)\right| d\tau \leq \sqrt{\int_u^s 1 d\tau \cdot \int_u^s \left|\dot{\vec{X}}(\tau)\right|^2 d\tau}$$

$$\gamma^2(s,u) \leq (s-u) \int_u^s \left|\dot{\vec{X}}(\tau)\right|^2 d\tau \tag{60}$$

$$\Delta D = 2\int_0^t \int_0^s J(s-u)\left(1-\cos\left(\gamma(s,u)\right)\right) duds =$$

$$= 4\int_0^t \int_0^s J(s-u)\sin^2\left(\frac{\gamma}{2}\right) duds \leq$$

$$\leq \int_0^t \int_0^s J(s-u)\gamma^2 duds \leq$$

$$\leq \int_0^t \int_0^s J(s-u) \left(\int_u^s \left| \dot{\vec{X}}(\tau) \right|^2 d\tau \right) (s-u)\, duds =$$

$$= \int_0^t ds \int_0^s J(y) \left(\int_{s-y}^s \left| \dot{\vec{X}}(\tau) \right|^2 d\tau \right) ydy =$$

$$= \int_0^t J(y)\, ydy \int_y^t ds \left(\int_{s-y}^s \left| \dot{\vec{X}}(\tau) \right|^2 d\tau \right) \leq$$

$$\leq \int_0^t J(y)\, y^2 dy \left(\int_0^t \left| \dot{\vec{X}}(\tau) \right|^2 d\tau \right) \leq$$

$$\leq \quad E \cdot \int_0^t J(y)\, y^2 dy \tag{61}$$

So any decoupling scheme's efficiency is limited by the amount of energy allowed for the control field.

10 Optimal square pulse

In this section we show how different constraints lead to different optimal square pulses - and that for the case of finite energy wide pulses are optimal. A square pulse, as the one described in section 6.4, has energy $\Omega^2 d = E_{pulse}$. Equation 44 can be expressed through this energy as:

$$D_{pulse}(d,t) = 2\nu^2\tau \left((t-d) + \frac{1}{\left(1 + \frac{E_{pulse}}{d}\tau^2\right)} d \right) = 2\nu^2\tau \left(t - d \left(\frac{1}{\left(1 + \frac{d}{E_{pulse}\tau^2}\right)} \right) \right) \tag{62}$$

Minimizing $D_{pulse}(d,t)$ in respect to E_{pulse}, it's clear that the optimal choice is $E_{pulse} \to \infty$ so the pulse will use all the available energy ($E_{pulse} = E$). Minimizing $D_{pulse}(d,t)$ in respect to d is equivalent to minimizing $\frac{1}{d} + \frac{1}{E\tau^2}$, which gives $d_{opt} \to \infty$ - translating in our case to $d_{opt} = t$. We see that for this case wide pulses are better than sharp ones.

This result might come as a surprise considering the multiple times we mentioned the importance of acting on the system faster than the noise correlation time length (τ). In the case of long and constant square pulses, the correct time scale that ought to be compared to τ is not the width of the pulse (d) but the Rabi frequency induced by it's intensity (or more accurately its inverse: $\frac{1}{\Omega}$). While there is no field - the "race" against τ is completely lost, when there is a constant field the race might be won or lost by a smaller margin - creating less decoherence than zero control. The total quality of the control scheme is determined by the average of these "race results" over the experiment time. By choosing the pulse width we decide whether we prefer beating τ by a large margin for a short time or beating it by a much smaller margin (or even losing but not totally) but for a longer time. Here we have shown that the best tradeoff is achieved by choosing the weaker but wider pulse.

Using a restriction on the total phase of the pulse ($\int_0^t \Omega(t)\,dt = \alpha \Rightarrow \Omega d = \alpha$) instead of total energy (for example if we want to determine the best shape of a π pulse) we can write:

$$D_{pulse}(d,t) = 2\nu^2\tau\left((t-d) + \frac{1}{\left(1+\left(\alpha\frac{\tau}{d}\right)^2\right)}d\right) = 2\nu^2\tau\left(t - \frac{1}{\frac{1}{d} + \frac{d}{(\alpha\tau)^2}}\right) \tag{63}$$

Minimizing $D_{pulse}(d,t)$ gives $d_{opt} = \alpha\tau$ - meaning a narrow pulse. Note that at this pulse width our assumption $\frac{d}{\tau} \gg 1$ is no longer true (it is reasonable to assume $\alpha \lesssim 2\pi$) - so we cannot state anything about the real optimal width except $d_{opt} \lesssim \alpha\tau$. So for constant phase - narrow pulses are better, exemplifying the difference between optimal control fields for different constraints.

11 Asymptotic optimality

In this part we show that for several asymptotical cases the constant control field achieves the upper bound from section 9, making it an optimal solution in these cases. Calculating the improvement in decoherence for the case of constant control field, using equation 41 for $\frac{t}{\tau} \gg 1$ and $t\Omega^2 = E$, we get:

$$\begin{aligned} \Delta D(t) &= 2\nu^2\tau t \cdot \left(1 - \frac{1}{(\Omega\tau)^2 + 1}\right) = \\ &= 2\nu^2\tau t\frac{1}{1 + \frac{t}{E\tau^2}} \end{aligned} \tag{64}$$

For the case of $\frac{t}{\tau} \gg E\tau$ this is equal to:

$$\Delta D = 2\nu^2 E\tau^3 \tag{65}$$

Remembering equation 61 we calculate the bound for $J(s) = \nu^2 e^{-\frac{|s|}{\tau}}$ ($\frac{t}{\tau} \gg 1$) using the "Mathematica" code:

```
Integrate[s^2*Exp[-s/τ], {s, 0, t}] ⟹
⟹ 2 τ^3 - E^(-(t/τ)) τ (t^2 + 2 t τ + 2 τ^2)
```

$$E \cdot \int_0^t J(y)\, y^2 dy = E \cdot 2\nu^2 \tau^3 \tag{66}$$

So we see that the CF DD scheme saturates the bound for fast noise ($\tau \to 0$), weak control ($E \to 0$) or long experiment times ($t \to \infty$) - making it one of the asymptotically optimal controls.

12 Summary

12.1 List of main results

- Formula of decoherence as a function of time, defined by the noise statistical properties and a general control field (derived using quantum channel properties and perturbation theory) - section 3.

- Higher perturbation order calculation via Feynman diagrams, convergence and upper bound on the n^{th} order - section 4.

- Geometric interpretation of the decoherence integral and its calculation - sections 3.1 and 6.

- Independent reproduction and improvement of the integro-differential equation for optimal control first presented in [35] (using Euler Lagrange formalism) - section 8.

- General upper bound on the purity improvement that can be achieved by any energy limited DD scheme - section 9.

12.2 Discussion

In this work we have discussed the problem of dynamically decoupling a 2 level system from its surrounding noise by applying an open-loop, energy constrained control. We gave geometric interpretation to the resulting decoherence equations and produced a graphical way of calculating the decoherence function for a general DD scheme. These tools can be used to visually compare or improve any type of DD - whether pulsed or general. Alternatively, one may use equation 57 to calculate numerically the best control scheme for a specific system.

Looking at specific cases, we have shown that DD can reverse the flow of entropy for noises with memory. We have seen that adding the energy constraint, especially for low energies, changes the rules of the game. The results in sections 10 and 11 hint (under certain conditions) toward optimal control fields that are wide and gradually changing, rather than the sharp π-pulses that are popular today. The bound derived in section 9 exemplifies the omnipresent truth: “there are no free lunches”. Translated to the language of DD it means that no matter how clever our choice of control scheme is, if we want to achieve substantial qubit lifetime extension - we have to pay in energy.

To conclude, the area of pulsed dynamic decoupling is well studied, both theoretically and experimentally. In contrast, there is relatively little theoretical work done in the area of energy restricted DD, and almost no experimental results. As we said, the general analytical problem is hard: there is no known solution to the optimal control equation from section 8 and it is unknown whether the solution is unique and stable (these questions remain open for future research). The generalization of both the noise and control field to more than one dimension is a natural extension of our work, but seems to be non-trivial under our formalism. Another important challenge that we did not address is control field errors (random fluctuations in the control field that are proportional to its intensity) - which is a dominant limitation on the quality of pulsed DD today.

A Channel eigenvalues

Following the definitions in 2.2 and discussion in 3, we are interested in calculating how far the channel's eigenvalues are from 1 (their absolute value to be exact - but since we are discussing the perturbative regime all eigenvalues are close to 1 so obviously positive). This definition of decoherence is equivalent to the trace distance of the decohering channel from the ideal one ($\mathcal{C}_{identity}\left[\vec{R}\right]=\vec{R}$):

$$D=Tr\left[\mathcal{C}_{identity}-\mathcal{C}\right]=\sum_{\vec{R}_i}\vec{R}_i\left(\mathcal{C}_{identity}-\mathcal{C}\right)\left[\vec{R}_i\right]$$

Where $\vec{R}_i$ are orthonormal basis vectors of the Bloch space. Arbitrarily choosing the $\hat{x}\,\hat{y}\,\hat{z}$ basis and using equation 16 we write:

$$D=\sum_{i=x,y,z}\vec{R}_i\left(\mathcal{C}_{identity}-\mathcal{C}\right)\left[\vec{R}_i\right]=$$

$$=\sum_{i=x,y,z}\vec{R}_i\cdot\left\{\vec{R}_i-\vec{R}_i-\int\limits_0^t\int\limits_0^s\left\langle\eta\left(s\right)\eta\left(u\right)\right\rangle\left[\left(\vec{X}\left(s\right)\cdot\vec{R}_i\right)\vec{X}\left(u\right)-\left(\vec{X}\left(s\right)\cdot\vec{X}\left(u\right)\right)\vec{R}_i\right]duds\right\}$$

$$=-\sum_{i=x,y,z}\int\limits_0^t\int\limits_0^s\left\langle\eta\left(s\right)\eta\left(u\right)\right\rangle\left[\left(\vec{X}\left(s\right)\cdot\vec{R}_i\right)\vec{R}_i\cdot\vec{X}\left(u\right)-\left(\vec{X}\left(s\right)\cdot\vec{X}\left(u\right)\right)\vec{R}_i\cdot\vec{R}_i\right]duds$$

$$=-\int\limits_0^t\int\limits_0^s\left\langle\eta\left(s\right)\eta\left(u\right)\right\rangle\sum_{i=x,y,z}\left[\left(\vec{X}\left(s\right)\cdot\vec{R}_i\right)\left(\vec{X}\left(u\right)\cdot\vec{R}_i\right)-\left(\vec{X}\left(s\right)\cdot\vec{X}\left(u\right)\right)\left|\vec{R}_i\right|^2\right]duds$$

$$=-\int\limits_0^t\int\limits_0^s\left\langle\eta\left(s\right)\eta\left(u\right)\right\rangle\left[\sum_{i=x,y,z}\vec{X}_i\left(s\right)\vec{X}_i\left(u\right)-\sum_{i=x,y,z}\left(\vec{X}\left(s\right)\cdot\vec{X}\left(u\right)\right)\right]duds$$

$$=-\int\limits_0^t\int\limits_0^s\left\langle\eta\left(s\right)\eta\left(u\right)\right\rangle\left[\vec{X}\left(s\right)\cdot\vec{X}\left(u\right)-3\vec{X}\left(s\right)\cdot\vec{X}\left(u\right)\right]duds$$

$$=2\int\limits_0^t\int\limits_0^s\left\langle\eta\left(s\right)\eta\left(u\right)\right\rangle\vec{X}\left(s\right)\cdot\vec{X}\left(u\right)duds$$

Which is exactly equation 17.

B Spectral form derivation

We start with the decoherence integral expressed using the window function:

$$W_t(s) = \begin{cases} 0 & s < 0 \\ 1 & 0 < s < t \\ 0 & t < s \end{cases}$$

$$f_t(s) = W_t(s) \cdot e^{i \int_0^s \Omega(\tau) d\tau}$$

$$\begin{aligned} D(t) &= \Re\left[\int_{-\infty}^{\infty}\int_{-\infty}^{\infty} J(s-u)\, f_t(s)\, \overline{f_t}(u)\, duds\right] = \\ &= \Re\left[\int_{-\infty}^{\infty} f_t(s)\left(J * \overline{f_t}\right)(s)\, ds\right] \end{aligned}$$

Since we assumed $J(s)$ is square integrable, it has a Fourier transform $\hat{J}(\omega)$. Using the convolution properties and Parseval's theorem we can write:

$$\begin{aligned} D(t) &= \Re\left[\int_{-\infty}^{\infty} f_t(s)\left(J * \overline{f_t}\right)(s)\, ds\right] = \\ &= \Re\left[\int_{-\infty}^{\infty} \bar{\hat{f_t}}(\omega)\left(J \hat{*} \overline{f_t}\right)(\omega)\, d\omega\right] = \\ &= \Re\left[\sqrt{2\pi}\int_{-\infty}^{\infty} \bar{\hat{f_t}}(\omega) \hat{J}(\omega)\, \hat{\overline{f_t}}(\omega)\, d\omega\right] = \\ &= \Re\left[\sqrt{2\pi}\int_{-\infty}^{\infty} \hat{J}(\omega)\left|\hat{\overline{f_t}}(\omega)\right|^2 d\omega\right] = \\ &= \sqrt{2\pi}\int_{-\infty}^{\infty} \hat{J}(\omega)\left|\hat{f_t}(\omega)\right|^2 d\omega \end{aligned}$$

Where in the end we used the fact that $J(s)$ is real and symmetric (so $\hat{J}(\omega)$ is real and symmetric). This is exactly equation 50.

C Optimal control: Euler-Lagrange

In order to solve the constrained minimization problem:

$$\begin{cases} \min_{\vec{X}} D(t) \\ \left|\vec{X}\right| = 1 \\ \int_0^t \left|\dot{\vec{X}}(s)\right|^2 ds \le E \end{cases}$$

the Euler-Lagrange variational technique can be used. In order to satisfy the demand $\left|\vec{X}(s)\right| = 1$ at all times, we take the variation in $\vec{X}$ to be perpendicular to it: $\delta\vec{X}(s) = \vec{v}(s) \times \vec{X}(s)$, where $|\vec{v}(s)|$ is small for any s. Rewriting the constraint for $\vec{X}(s) \to \vec{X}(s) + \delta\vec{X}(s)$:

$$\frac{d\left(\delta\vec{X}(s)\right)}{ds} = \dot{\vec{v}}(s) \times \vec{X}(s) + \vec{v}(s) \times \dot{\vec{X}}(s)$$

$$\begin{aligned} & \int_0^t \left|\frac{d\left(\vec{X}(s) + \delta\vec{X}(s)\right)}{ds}\right|^2 - \left|\dot{\vec{X}}(s)\right|^2 ds = \\ = \; & 2\int_0^t \dot{\vec{X}}(s) \cdot \left(\dot{\vec{v}}(s) \times \vec{X}(s) + \vec{v}(s) \times \dot{\vec{X}}(s)\right) ds = \\ = \; & 2\int_0^t \dot{\vec{v}}(s) \cdot \left(\vec{X}(s) \times \dot{\vec{X}}(s)\right) ds = \\ = \; & 2\vec{v}(s) \cdot \left(\vec{X}(s) \times \dot{\vec{X}}(s)\right) |_0^t - 2\int_0^t \vec{v}(s) \cdot \frac{d\left(\vec{X}(s) \times \dot{\vec{X}}(s)\right)}{ds} ds = \\ = \; & 2\vec{v}(s) \cdot \left(\vec{X}(s) \times \dot{\vec{X}}(s)\right) |_0^t - 2\int_0^t \vec{v}(s) \cdot \left(\vec{X}(s) \times \ddot{\vec{X}}(s)\right) ds \end{aligned}$$

The end points force the condition:

$$\vec{X}(0) \times \dot{\vec{X}}(0) = \vec{X}(t) \times \dot{\vec{X}}(t) = 0$$

While the integral part is the constraint written in variational form. Now calculating δD (using equation 18 and $\cos(\gamma(s,u)) = \vec{X}(s)\cdot\vec{X}(u)$):

$$D(t) = \int_0^t \int_0^t J(s-u)\left(\vec{X}(s) + \delta\vec{X}(s)\right)\cdot\left(\vec{X}(u) + \delta\vec{X}(u)\right) duds$$

$$\begin{aligned}\delta D(t) &= \int_0^t \int_0^t J(s-u)\left(\vec{X}(s)\cdot\left(\vec{v}(u)\times\vec{X}(u)\right) + \vec{X}(u)\cdot\left(\vec{v}(s)\times\vec{X}(s)\right)\right) duds = \\ &= 2\int_0^t \int_0^t J(s-u)\,\vec{X}(u)\cdot\left(\vec{v}(s)\times\vec{X}(s)\right) duds\end{aligned}$$

Putting the two calculations together we get:

$$\int_0^t \int_0^t J(s-u)\,\vec{v}(s)\cdot\left(\vec{X}(s)\times\vec{X}(u)\right) duds = \lambda\int_0^t \vec{v}(s)\cdot\left(\vec{X}(s)\times\ddot{\vec{X}}(s)\right) ds \Longrightarrow$$

$$\Longrightarrow \vec{X}(s)\times\left[\int_0^t J(s-u)\,\vec{X}(u)\,du - \lambda\ddot{\vec{X}}(s)\right] = 0$$

Which is exactly equation 57.

References

[1] M. A. Nielsen and I. L. Chuang. “Quantum Computation and Quantum Information”, Cambridge University Press, Cambridge, 2000.

[2] Bennett, Charles H., and David P. DiVincenzo. "Quantum information and computation." Nature 404.6775 (2000): 247-255.

[3] Zurek, Wojciech H. "Decoherence and the transition from quantum to classical–REVISITED." arXiv preprint quant-ph/0306072 (2003).

[4] Medintz, Igor L., et al. "Quantum dot bioconjugates for imaging, labelling and sensing." Nature materials 4.6 (2005): 435-446.

[5] Mamin, H. J., et al. "Nanoscale Nuclear Magnetic Resonance with a Nitrogen-Vacancy Spin Sensor." Science 339.6119 (2013): 557-560.

[6] Taylor, J. M., et al. "High-sensitivity diamond magnetometer with nanoscale resolution." Nature Physics 4.10 (2008): 810-816.

[7] Staudacher, T., et al. "Nuclear Magnetic Resonance Spectroscopy on a (5-Nanometer) 3 Sample Volume." Science 339.6119 (2013): 561-563.

[8] Hirose, Masashi, Clarice D. Aiello, and Paola Cappellaro. "Continuous dynamical decoupling magnetometry." arXiv preprint arXiv:1207.5729 (2012).

[9] Buluta, Iulia, and Franco Nori. "Quantum simulators." Science 326.5949 (2009): 108-111.

[10] Cai, Jianming, et al. "Towards a large-scale quantum simulator on diamond surface at room temperature." arXiv preprint arXiv:1208.2874 (2012).

[11] Bennett, Charles H., et al. "Mixed-state entanglement and quantum error correction." Physical Review A 54.5 (1996): 3824.

[12] Viola, Lorenza, Emanuel Knill, and Seth Lloyd. "Dynamical decoupling of open quantum systems." Physical Review Letters 82.12 (1999): 2417-2421.

[13] Viola, Lorenza, and Seth Lloyd. "Dynamical suppression of decoherence in two-state quantum systems." Physical Review A 58.4 (1998): 2733.

[14] Hahn, Erwin L. "Spin echoes." Physical Review 80.4 (1950): 580.

[15] Carr, Herman Y., and Edward M. Purcell. "Effects of diffusion on free precession in nuclear magnetic resonance experiments." Physical Review 94.3 (1954): 630.

[16] Meiboom, S., and D. Gill. "Modified spin echo method for measuring nuclear relaxation times." Review of Scientific Instruments 29.8 (1958): 688-691.

[17] Gullion, Terry, David B. Baker, and Mark S. Conradi. "New, compensated carr-purcell sequences." Journal of Magnetic Resonance (1969) 89.3 (1990): 479-484.

[18] Khodjasteh, K., and D. A. Lidar. "Fault-tolerant quantum dynamical decoupling." Physical review letters 95.18 (2005): 180501.

[19] Uhrig, Götz S. "Keeping a quantum bit alive by optimized π-pulse sequences." Physical review letters 98.10 (2007): 100504.

[20] Uhrig, Götz S., and Daniel A. Lidar. "Rigorous bounds for optimal dynamical decoupling." Physical Review A 82.1 (2010): 012301.

[21] Pasini, Stefano, and Götz S. Uhrig. "Optimized dynamical decoupling for time-dependent Hamiltonians." Journal of Physics A: Mathematical and Theoretical 43.13 (2010): 132001.

[22] Uhrig, Götz S. "Exact results on dynamical decoupling by π-pulses in quantum information processes." New Journal of Physics 10.8 (2008): 083024.

[23] Uhrig, Götz S. "Concatenated control sequences based on optimized dynamic decoupling." Physical review letters 102.12 (2009): 120502.

[24] Biercuk, M. J., A. C. Doherty, and H. Uys. "Dynamical decoupling sequence construction as a filter-design problem." Journal of Physics B: Atomic, Molecular and Optical Physics 44.15 (2011): 154002.

[25] Wang, Zhi-Hui, et al. "Comparison of dynamical decoupling protocols for a nitrogen-vacancy center in diamond." Physical Review B 85.15 (2012): 155204.

[26] Yang, Wen, Zhen-Yu Wang, and Ren-Bao Liu. "Preserving qubit coherence by dynamical decoupling." Frontiers of Physics 6.1 (2011): 2-14.

[27] Kuo, W-J., et al. "*Universality* proof and analysis of generalized nested Uhrig dynamical decoupling." arXiv preprint arXiv:1207.1665 (2012).

[28] West, Jacob R., Bryan H. Fong, and Daniel A. Lidar. "Near-optimal dynamical decoupling of a qubit." Physical review letters 104.13 (2010): 130501.

[29] Khodjasteh, Kaveh, and Daniel A. Lidar. "Performance of deterministic dynamical decoupling schemes: Concatenated and periodic pulse sequences." Physical Review A 75.6 (2007): 062310.

[30] Pasini, S., et al. "Optimized pulses for the perturbative decoupling of a spin and a decoherence bath." Physical Review A 80.2 (2009): 022328.

[31] Kofman, A. G., and G. Kurizki. "Universal dynamical control of quantum mechanical decay: modulation of the coupling to the continuum." Physical review letters 87.27 (2001): 270405.

[32] Gordon, Goren, Noam Erez, and Gershon Kurizki. "Universal dynamical decoherence control of noisy single-and multi-qubit systems." Journal of Physics B: Atomic, Molecular and Optical Physics 40.9 (2007): S75.

[33] Viola, Lorenza, and Emanuel Knill. "Robust dynamical decoupling of quantum systems with bounded controls." Physical review letters 90.3 (2003): 37901.

[34] Clausen, Jens, Guy Bensky, and Gershon Kurizki. "Bath-optimized minimal-energy protection of quantum operations from decoherence." Physical review letters 104.4 (2010): 40401.

[35] Gordon, Goren, Gershon Kurizki, and Daniel A. Lidar. "Optimal dynamical decoherence control of a qubit." Physical review letters 101.1 (2008): 10403.

[36] Fujiwara, Akio, and Paul Algoet. "One-to-one parametrization of quantum channels." Physical Review A 59.5 (1999): 3290.

[37] Isserlis, Leon. "On a formula for the product-moment coefficient of any order of a normal frequency distribution in any number of variables." Biometrika 12.1/2 (1918): 134-139.

[38] Bogoljubov, Nikolaj N., et al. “Introduction to the theory of quantized fields”. Interscience publishers, 1959.

[39] Klauder, J. R., and P. W. Anderson. "Spectral diffusion decay in spin resonance experiments." Physical Review 125.3 (1962): 912.

[40] Timoney, N., et al. "Quantum gates and memory using microwave-dressed states." Nature 476.7359 (2011): 185-188.

בקרה של מערכת 2 רמות למזעור רעש צבוע

מיכאל שליט

בקרה של מערכת 2 רמות למזעור רעש צבוע

חיבור על מחקר

לשם מילוי חלקי של הדרישות לקבלת התואר
מגיסטר למדעים בפיסיקה

מיכאל שליט

הוגש לסנט הטכניון - מכון טכנולוגי לישראל

שבט תשע"ג חיפה ינואר 2013

המחקר נעשה בהנחיית פרופסור יוסף אברון בפקולטה לפיסיקה.

אני מודה לפרופסור אברון על ההזדמנות שהוא נתן לי, על רוחו ושיעוריו לחיים.

אני מודה לד"ר אלכס רצקר על הצעתו לנושא מחקר, הנחיתו ותמיכתו.

אני מודה לד"ר עודד קנת' על תרומתו למחקר.

אני מודה להורי על תמיכתם, אהבתם ואמונתם בי.

אני מודה לאוניברסיטת אולם על הכנסת האורחים והתמיכה הכספית הנדיבה בזמן ביקורי.

אני מודה לטכניון ולקרן הלאומית למדע על התמיכה הכספית הנדיבה בהשתלמותי.

תקציר

הפוטנציאל הגלום במערכות המתנהגות לפי חוקי הפיזיקה הקוונטית לביצוע חישובים במהירות העולה באופן איכותי על האפשרי במערכות קלאסיות, הניע את עליית העיניין באינפורמציה קוונטית ומחשוב קוונטי ב־20 שנה האחרונות. קריפטוגרפיה קוונטית, תקשורת קוונטית, מדידת שדות מגנטיים באופן מדויק, חישה של מערכות ביולוגיות בעזרת התקנים קונטיים מיקרוסקופיים וסימולציות של תאוריות מדעיות ־ כל אלו הם רק חלק מהשימושים המתאפשרים ע"י שליטה קוהרנטית במערכת קוונטית. לרוע המזל, כל מערכת פיזיקלית מצומדת לסביבתה במידה זו או אחרת, צימוד זה שוזר את המצב הקוונטי של המערכת עם המצב של הסביבה. היות והסביבה לא נגישה לנו ומצבה לא ידוע, שזירה זו יוצרת זליגת מידע מהמערכת ־ מה שמגדיל את האי־וודאות הקלאסית, משמע האנתרופיה, והופך את מצב המערכת מטהור למעורבב. ככל שהאנתרופיה של המצב הולכת וגדלה, כך המערכת מאבדת את תכונותיה הקוונטיות ומתנהגת יותר ויותר באופן קלאסי ־ מה שמונע את כל אותם השימושים שהוזכרו.

דרך אפשרית אחת להלחם באובדן הקוהרנטיות היא לבודד את המערכת עד כמה שניתן מהסביבה, ולרוב במערכות ניסיוניות מקדישים לא מעט תשומת לב לנושא, אך לעיתים לא ניתן להגיע בשיטה זו להגנה הרצויה. שיטה אלטרנטיבית היא "הפרדה דינמית" ־ הפעלת שדה בקרה אקטיבי הפועל על המערכת בלבד, באופן דטרמיניסטי, ומקטין את האינטרקציה האפקטיבית בין המערכת לסביבתה. הרעיון מאחורי השיטה הותאם למערכות קוונטיות מהתחום של NMR, שם משתמשים בפולסי בקרה חדים כדי להתגבר על אי־הומוגניות באמבט ספינים כבר למעלה מ־60 שנה. לעומת זאת, במערכות קוונטיות ־ בהן לרוב מדובר על ספינים בודדים ־ שיטת ההפרדה הדינמית צברה פופולריות רק ב־15־10 שנה האחרונות. הפרטים של שדה הבקרה (קרי כמות, תזמון, פאזת ועוצמת הפולסים) ויעילותו נחקרו לעומק בעשור האחרון והוצעו מספר סכמות בקרה עיקריות ־ אשר מתבססות על מדדי איכות שונים ־ והאפקטיביות שלהן נמדדה נסיונית.

לעומת כל האמור, הפרדה דינמית אשר לא מתבססת על פולסים ־ קרי שדה בקרה כללי אשר משתנה בזמן ־ כמעט ולא נחקר. מספר חוקרים התייחסו לפולסים מציאותיים ־ משמע סופיים בעוצמתם ומשכם ־ אך כמעט ולא היתה היתייחסות לשדה בקרה אשר לא מתבסס על סכמה פולסית. סיטואציה פיזיקלית אפשרית אחת אשר מכריחה התייחסות כזו היא כאשר האנרגיה הכללית שמותר להפעיל על המערכת מוגבלת. הגבלת אנרגיה כזו יכולה לעלות מהצורך למנוע חימום יתר של המערכת (למשל בניסויי חישה של מערכות ביולוגיות) או מאי

דיוקים בשדה הבקרה עצמו (מה ששקול להוספת רעש למערכת), שאז נרצה להקטין את השדה המופעל ככל הניתן. בעבודה זו נחקר מנגנון ההפרדה הדינמית תחת הגבלת האנרגיה של שדה הבקרה הכולל.

המודל בו אנו משתמשים הוא מערכת 2 רמות (קיוביט - למשל 2 המצבים של ספין $\frac{1}{2}$) אשר מופרדות אנרגטית ע"י שדה מגנטי קבוע (היוצר הפרדה ω_0) ושדה נוסף המשתנה בזמן ($\eta\left(t\right)$) בעל ממוצע 0. שדה זה נוצר ע"י פלקטואציות מגנטיות של הסביבה ואינו ידוע לנו - לכן נחשוב עליו בתור רעש. בנוסף, על הקיוביט פועל שדה בקרה כלשהו המסובב את מצבו באופן אוניטרי (קוהרנטי) בספרת בלוך. סיבוב זה משנה את השפעת הרעש (במובן מסויים ממצע אותו) אבל "עולה" האנרגיה. בשלב הראשון אנו מפתחים נוסחה להתפתחות בזמן של הקיוביט במערכת הייחוס המסתובבת עם השפעת שדה הבקרה, בעזרת פיתוח הפרעתי עד לסדר שני (הסדר הלא טריוויאלי המוביל). אנו מגדירים ערוץ קוונטי אשר מקדם את המצב ההתחלתי של המערכת למצב בזמן t כלשהו, בעזרת תכונותיו אנו מגדירים מדד לאובדן קוהרנטיות ומחשבים מפורשות את הפונקציה המגדירה אותו בתלות בשדה הבקרה והאוטוקורלציה של הרעש. לנוסחה זו יש פירוש גאומטרי פשוט בו אנו דנים בקצרה.

כהרחבה לפיתוח ההפרעתי לסדר שני, בעיית חישוב הסדרים הגבוהים יותר הומרה לשאלת חישוב דיאגרמות פיינמן. תרגום זה מאפשר שימוש בכלים המתמטיים הנרחבים שפותחו לאורך השנים בתחום תורת השדות הקוונטית, ובאופן עקרוני לחשב את תרומת כל סדר בפיתוח ההפרעתי. בנוסף, אנו מפתחים צורה ספקטרלית של פונקציית אובדן הקוהרנטיות - אשר מתייחסת לספקטרום הרעש ולחלון התדירויות האפקטיבי ששדה הבקרה יוצר, מה שמתרגם את השאלה לבעיית תכנון פילטרים קלאסית.

בהמשך אנו מוסיפים באופן פורמלי את הגבלת האנרגיה על שדה הבקרה ומנסחים בעיית אופטימיזציה. בעזרת חישוב וואריאציות (שיטת אויילר לגראנג') אנו מפתחים משוואה אינטגרו-דיפרנציאלית לא לינארית עבור שדה הבקרה האופטימלי (בהינתן האנרגיה המקסימלית ותכונות הרעש). לרוע המזל, משוואה זו קשה לפיתרון באופן כללי, לכן התמקדנו בדוגמאות פרטיות ותכונות כלליות של המודל. בשלב הראשון חושב חסם עליון על כמות השיפור שיכולה להביא כל סכמת בקרה מוגבלת אנרגטית לעומת העדר בקרה (ההפרש בין אובדן הקוהורנטיות כאשר מופעל שדה הבקרה לאובדן כאשר הוא כבוי - במהלך אותו משך זמן). החסם תלוי לינארית באנרגיה, משמע בהינתן אנרגיה מקסימלית ורעש מסוים - אף סכמת בקרה לא תוכל להיות יעילה באופן שרירותי. תכונה זו מדגימה את האמירה הידועה "אין ארוחות חינם": אם רוצים שיפור משמעותי בקוהורנטיות המערכת בעזרת הפרדה דינאמית - חייבים לשלם באנרגיה.

לאחר מכן אנו בוחנים מספר מקרים פרטיים (בעזרת שיטה גרפית לויזואליזציה של אינטגרל אובדן הקוהרנטיות):

- עבור המקרה של אמבט חסר זכרון (משמע פונקציית אוטוקורלציה דמויית $\gamma(t)$ - רעש לבן), אנו מוכיחים כי אובדן הקוהורנטיות מתרחש בקצב קבוע - ללא תלות בפרטי שדה הבקרה המופעל (כולל העדר בקרה כלל). תוצאה זו מראה את התלות של הצלחת הפרדה דינאמית באורך זכרון הרעש: הבקרה חייבת לבצע שינויים במערכת מהר יותר מקצב השתנות הרעש - כאשר הבקרה איטית מדי ביחס לרעש (כמו במקרה של אורך זכרון אפסי) השיטה אינה מצליחה להגן על קוהורנטיות המצב.
- במקרה של רעש בעל ספקטרום לורנצי (אוטוקורלציה דועכת אקספוננציאלית) ניתן לחשב את פונקציית אובדן הקוהורנטיות ללא שדה בקרה (התפתחות חופשית) ולראות כי היא עולה באופן ריבועי בזמן.
- בעזרת הפורמליזם שפיתחנו ניתן להבין את שיטת ההפרדה הדינמית הפשוטה ביותר ב- NMR, הד ספיני. אנו רואים שפולס יחיד מאריך את זמן החיים של המערכת בפרק זמן מסדר גודל של אורך זיכרון המערכת, מה שמדגים את חשיבות זמן הקורלציה של הרעש ביעילות ההפרדה הדינמית.
- דוגמא נוספת היא שדה בקרה קבוע בזמן. שם אנו רואים כי יעילות ההגנה מרעש עולה עם כמות המחזורים שמספיק שדה הבקרה ליצור במצב הקיוביט בזמן אורך זכרון הרעש.
- דוגמא פרטית אחרונה שאנו בוחנים היא פולס בקרה רחב, אחיד בעוצמתו, באורך d. מנוסחת אובדן הקוהרנטיות אשר אנו מפתחים למקרה זה, אנו מראים כי במקרה של בקרה מוגבלת באנרגיה רוחב הפולס האופטימלי הוא הכי גדול שניתן (משמע $d=t$).

לבסוף, אנו משתמשים בנוסחה לאובדן קוהרנטיות עבור שדה קבוע בזמן ומשווים אותה לנוסחה עבור אובדן קוהרנטיות ללא שדה בקרה כלל (הכל למקרה הפרטי של רעש לורנצי). השוואה זו זהה לצורה בה קיבלנו את החסם העליון על כמות השיפור, לכן אנו משווים בין ההפרש לבין החסם ורואים שבמקרים גבוליים מסויימים שדה הבקרה הקבוע מרווה את החסם. רוויה זו מתרחשת בגבול של אנרגיה מקסימלית קטנה מאוד, זמן אבולוציה ארוך מאוד (שאז האנרגיה הכוללת חייבת להיות מפוזרת על פני זמן רב) או זמן קורלציית רעש קצר מאוד. בכל הסיטואציות הנ"ל ההפרדה הדינמית מספקת הגנה מואטה בלבד - אך את הרווח שאפשרי להשיג בשיטה זו ניתן להשיג בעזרת שדה בקרה קבוע בזמן.